Utrecht University

MAJOR INTERNSHIP REPORT

FUNCTIONAL CHARACTERIZATION OF CENTRIOLAR PROTEINS CEP120 AND SPICE1

TESSA VREMAN (6270565)

Molecular and Cellular Life Sciences

Graduate School of Life Sciences

Utrecht University

EXAMINER: Prof. Dr. A.S. Akhmanova

SECOND REVIEWER: Dr. Florian Berger

SUPERVISOR: Dr. F.E. Ogunmolu

DECEMBER 2021

Layman's summary

Animal cells have a cytoskeleton that gives them their shape and structure, just like the skeleton does with a whole organism. The cytoskeleton consists of three components: actin filaments, intermediate filaments and microtubules. All three components have a slightly different function, but we will focus on the microtubules in this study. As the name says, microtubules are small, hollow tubes. They are formed by the protein tubulin and stretch throughout the cell to form a network. Besides their structural function, microtubules are also important in intracellular transport. The microtubule network is organized by a small structure called the centrosome. This centrosome is located near the nucleus of the cell, and from there, the microtubules extend through the whole cell.

The centrosome is formed by two centrioles that are arranged perpendicularly. Centrioles are cylinders built from microtubules and centriolar proteins. The centrioles are approximately 500 nm long in human cells. Centriolar proteins are proteins that are located at the centrioles and perform their function there. The structure of the centrosome is crucial for the microtubules to be able to grow and form the network as they should. Besides the centrosome's normal function in the cell, it also has a role in mitosis. During cell division, the centrosome is duplicated and the two centrosomes form the mitotic spindles that help divide the genome evenly over the two cells. If there is a problem with genome distribution, this can lead to issues with the newly formed cells or even cancer. There are also diseases that are caused by poorly or non-functioning centrosomes, and more specifically, problems with the centriolar proteins. Because issues with the centrosome can have disastrous results, it is vital to understand their function better. A better understanding of the centrosome could help treat diseases caused by issues with the centrosome.

After each cell division, the centrosome needs to be duplicated because each daughter cell only receives one centrosome consisting of two centrioles. For a new centrosome to form, two new centrioles need to grow from the two existing centrioles. This duplication happens during a process called centriole biogenesis. It is important that this process goes well since two functioning centrosomes are crucial for further cell divisions and the functioning of the daughter cells. The centrosomal proteins mentioned before are also involved during centrosome biogenesis. The centrosome cannot assemble and thus function properly without the centriolar proteins. However, there are many different centriolar proteins and not for all of them, their role in centriole biogenesis is uncovered. In this study, we look at two centrosomal proteins called CEP120 and SPICE1. Of these two proteins, the function in the centrosome is not entirely clear yet. With different experimental techniques, we will try to elucidate the role of CEP120 and SPICE1 in the centrosome. We used the fluorescent proteins GFP and mCherry to visualize the two proteins of interest. In this way, we can observe them under a microscope and analyze their behavior. We found effects and interactions of CEP120 and SPICE1 that could be important in centriole biogenesis.

Table of Contents

Abstract

The centrosome is the main microtubule-organizing center in animal cells and is essential for the structure and function of the microtubule network. It also has an important role in chromosome segregation and cilium formation. The centrosome is built from a pair of centrioles surrounded by centriolar proteins. The centriole structure is preserved and very important for its function. During centriole biogenesis, many centriolar proteins are involved in building the well-defined architecture of the centriole. However, the mechanism for how the centriolar proteins actuate this well-defined architecture is mostly unknown. Two such centriolar proteins with limited descriptions are the "Centrosomal protein of 120 kDa" (CEP120) and the "Spindle and centriole associated protein 1" (SPICE1). Here, we studied the behavior of CEP120 and SPICE1 both in a cellular environment and in in vitro reconstitution experiments. We found that CEP120 didn't bind to the microtubule network both in cells and in vitro, but we saw it bind to free tubulin in the in vitro reconstitution assays. In contrast, SPICE1 binds to microtubules both in cells and in reconstitution assays. Furthermore, SPICE1 stabilizes microtubules, which could be essential for its function in centriole biogenesis. Lastly, we looked at CEP120 and SPICE1 together and saw that SPICE1 did recruit CEP120 to the microtubules. In conclusion, we saw a stabilizing effect of SPICE1 and an interaction between CEP120 and SPICE1 that could play a role in centriole biogenesis.

Introduction

The centriole is an astounding and important microtubule-based structure that plays a crucial role in various cellular processes, including cilium biogenesis and chromosome segregation during cell division (Bornens, 2012; Kellog et al., 1994). Centrioles have a cylindrical shape with ninefold symmetry and well-defined length. Together with a matrix of pericentriolar material (PCM), two centrioles form a centrosome (Winey & O'Toole, 2014). The centrosome structure and function is well conserved between related species (Azimzadeh, 2014). It functions as the main microtubule-organizing center in most eukaryotic cells (Wu & Akhmanova, 2017). The microtubule network is of great importance in the eukaryotic cell. It not only provides structure and shape, it is also involved in intracellular transport, formation of cilia and flagella, and mitosis and meiosis (Nogales, 2001). The centrosome can also transform into the basal body, needed for cilia formation. After cell division, the centrioles need to be duplicated. The duplication is a tightly regulated process during which the centriole needs to grow very slowly to a well-defined length (Azimzadeh & Marshall, 2010). However, over a century after the discovery of the centrosome, the mechanism for its biogenesis is still only partly understood. Mainly the exceptionally slow growth rate of the centriolar microtubules and tightly regulated length of the centriole are important but not completely uncovered processes. Many different proteins are involved in regulating these processes and understanding their working mechanism is key to understanding the complex biogenesis of the centriole.

Centriole structure and function

For a long time, and sometimes still, the centrioles are depicted as just a dot near the nucleus of the cell. But in reality, there is a complex multiprotein structure where all the proteins have to fulfill their functions correctly for the centriole to perform its essential functions. Studying the centriole and the involved proteins is made more complicated by the fact that the size of the centrioles is just at the diffraction limit of conventional light microscopy. This meant that the centriole's underlying structure and protein localization remained unclear for a long time after its discovery. But with the help of electron microscopy and super-resolution microscopy, increasingly more is known about the centriole structure and the associated proteins. Furthermore, centriolar proteins have been hard to purify, partly because they are not expressed at high levels in the cell. Purifying proteins is needed, for example, to uncover a protein's structure with crystallography and for functional assays. All this has made it that the function and localization of centriolar proteins are still not entirely resolved.

Like with many cellular components, the importance of the centriole becomes apparent when it is removed. For example, when fertilization occurs without the necessary centriole supplied by the sperm. In this experiment with a *Xenopus leavis* oocyte, the oocyte can proceed through several rounds of the cell cycle but can't divide at the end of each cycle. Therefore, the oocyte can't develop into an embryo (Klotz et al., 1990). Additionally, loss or reduced function of the centrioles can lead to incomplete chromosome segregation or problems with cilia formation. Deregulation of centriole numbers also has long been thought to contribute to genome instability. Incomplete chromosome segregation is a known risk factor in cancer formation (Boveri, 2008; Nigg & Raff, 2009). Furthermore, mutations in specific centriolar proteins can have other pathological phenotypes for which the mechanism is not fully understood. This all indicates the importance of centrioles in cellular function and uncovering their structure.

As mentioned above, the centrosome also plays a role in the formation of cilia. Cilia are microtubule-based, hairlike cellular protrusions. The centrosome can transform into a basal body which forms the base of the cilia. The centrosome and basal body share the same basic structure and differ mainly in their function. Because the basal body and the centrosome are so alike in their structure, investigating the proteins of the centrosome can also be important for understanding the basal body better. Since problems with the basal body can lead to ciliopathies, disorders caused by dysfunctional cilia, it is important to understand the underlying mechanism better. Most ciliopathies

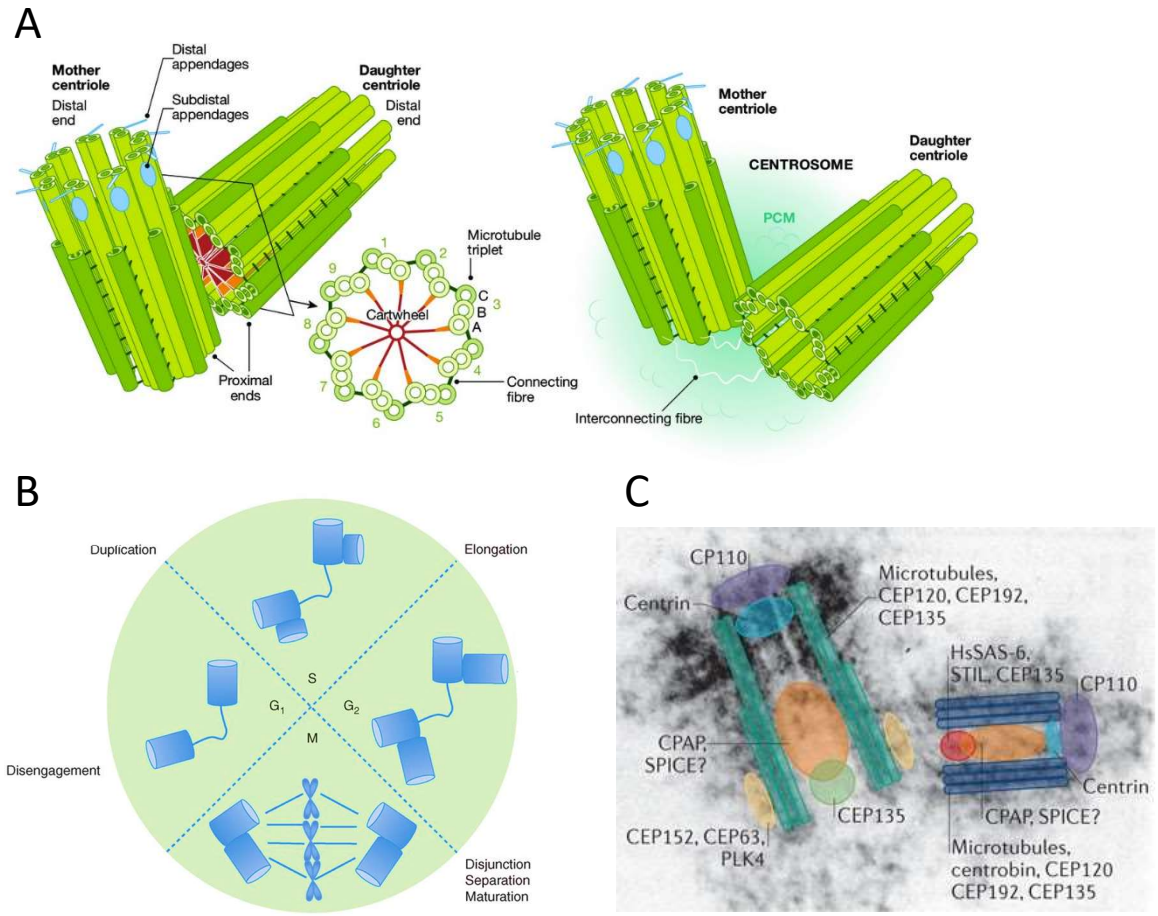

Figure 1. A schematic representation of the centrosome structure, biogenesis, and localization of centriolar proteins. (A) A schematic representation of the centrosome. (left) The two centrioles (mother and daughter), perpendicularly arranged. In green, the individual microtubules, arranged in triplets, and in darker green, the outer microtubules. The distal and subdistal appendages are depicted in light blue. (middle) The cartwheel structure in red and orange arranges the microtubule triplets into a cylindrical shape. (right) The complete centrosome with two centrioles connected by the interconnecting fibre and surrounded by the PCM. Adapted from Schatten & Simerly, 2015. (B) The centriole biogenesis during the cell cycle. Key events in the centriole cycle are indicated. Adapted from Fu et al., 2015. (C) An electron microscopy image of the human centrosome overlayed with the positions of its key proteins. Adapted from Gönczy, 2012 and Paintrand et al., 1992.

arise from a genetic defect in one or more centriolar proteins (Hildebrandt et al., 2011). Therefore, it is essential to understand the function and mechanism of these centriolar proteins.

Centrioles are arranged perpendicularly and are surrounded by the PCM (Figure 1A). A centriole is built from nine triplets of microtubules organized in a cylindrical shape by a cartwheel structure. The microtubules in the triplet are labeled A-C, with the inner microtubule being microtubule A. Although the centriole is a very conserved structure, there are slight differences between species and cell types (Silflow & Lefebvre, 2001). The typical human centriole has a diameter of approximately 250 nm and is 500 nm long (Winey & O'Toole, 2014). The two centrioles differ in age as a consequence of their biogenesis. After cell division, two new centrioles grow from the old centrioles (Figure 1B). The older centriole, called the mother centriole, is recognizable by the distal and subdistal appendages and is formed at least one cell cycle before the younger centriole, which is called the daughter centriole. The distal appendages can attach the centriole to the cell membrane, while the subdistal appendages form microtubule nucleation sites (Uzbekov & Alieva, 2018). These two centrioles form the basic structure around which all other centriolar proteins work. The PCM that

surrounds the two centrioles consists of many different proteins and has an essential role in the function of the centriole. These proteins mainly mediate protein-protein interactions that are important for the centriole function, for example, microtubule nucleation.

As mentioned above, the two centrioles passed down to the daughter cell have to grow a new centriole after each cell division (Figure 1B). This is a tightly regulated process because the centriole has to grow to an exact, well-defined length. The new centriole polymerizes at a very slow rate compared to the more dynamic cytoplasmic microtubules. Centrioles add only a few tubulin subunits per protofilament per hour. This rate is about 10,000 times slower than the cytoplasmic microtubules (Slep, 2016). Many regulating proteins are involved in this tightly regulated process that produces centrioles of a well-defined length. Uncovering their role and mechanism is the basis of a better understanding of centriole biogenesis.

Many different proteins involved in the structure and function of the centriole have been identified by mass spectrometry analysis and proteomic analysis (Banterle & Gönczy, 2017). They all seem to have a determined place on the centriole where they exert their function. Some of the proteins are located on the microtubules of the centriole, while others form structures around it (Figure 1C). For example, the centriolar protein CPAP binds and caps microtubule plus ends, and its activity decreases microtubule growth and stabilizes microtubules (Sharma et al., 2016). This capping by CPAP is essential to limit the growth of centriolar microtubules and thereby contributes to centriole length control. The centriolar protein CP110 is also involved in capping and limiting centriole extension (Schmidt et al., 2009). Another example is CEP135, a centriolar protein essential for cartwheel formation (Ohta et al., 2002; Roque et al., 2012). The cartwheel formation is a crucial step in centriole biogenesis. All in all, centriole biogenesis is orchestrated by specific centriolar proteins that each function in reaching the centrioles' well-defined length.

Despite the progress in centriolar research, we do not entirely understand the localization and function of all identified centriolar proteins. For example, the protein SPICE1 has a question mark behind it in Figure 1C because its location is not completely uncovered yet. Similarly, there are many other proteins with purported roles in centriole biogenesis but no clear mechanistic insights on the individual or combinatorial functions, as is the case for CEP120. Overall, the centriole is an essential and complex microtubule-organizing structure. Already its conservation through most eukaryotic cells and organisms indicates its importance. Furthermore, numerous disease genes encode centriolar proteins. Understanding the function and mechanism of these proteins will help uncover the working of the centriole in healthy cells and enable finding therapies for when the non-functional centriole causes pathologies.

The role of CEP120 in centriole biogenesis

The centrosomal protein of 120 kDa (CEP120) is a protein involved in centriole biogenesis and function. The importance of CEP120 is made clear by the fact that mutations of CEP120 cause complex ciliopathy phenotypes in humans, including Joubert syndrome and Jeune asphyxiating thoracic dystrophy. To understand how mutations in CEP120 cause these conditions in humans, it is crucial to understand the role and mechanism of CEP120 in centriole biogenesis. Previous studies have shown that loss of CEP120 causes short centriolar microtubules and, conversely, overexpression of the protein leads to overly elongated centrioles (Comartin et al., 2013; Lin et al., 2013; Tsai et al., 2019). It was found that the N-terminal domain of CEP120 can bind to cytoplasmic microtubules and is thus a microtubule-binding domain. Since CEP120 has this microtubule-binding domain, it is thought to be localized on the microtubules of the centriole (Figure 1C). CEP120 also has a domain through which it can interact with another known centriolar protein, CPAP (Lin et al., 2013). CPAP is also involved in centriole elongation. Overexpression of CPAP, like overexpression of CEP120, leads to overly elongated centrioles. However, for CPAP, there is a working model of its mechanism (Sharma et al., 2016), whereas the mechanism of CEP120 is still unknown. Part of the structure of CEP120 was uncovered, and this revealed the three C2 domains (C2A, C2B, and C2C) on its N-terminus (Joseph et al., 2018; Sharma et al., 2018). C2

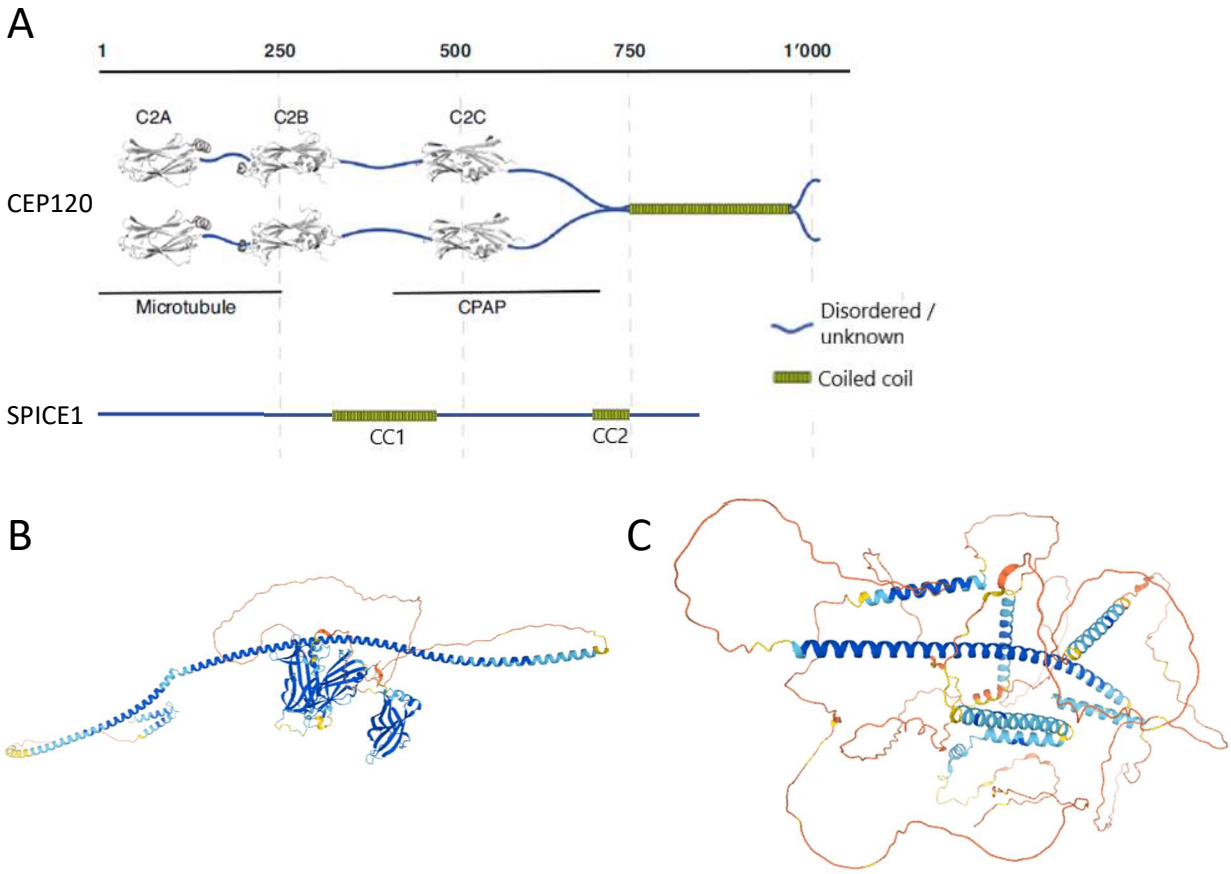

Figure 2. The secondary and tertiary structure of CEP120 and SPICE1. (A) The schematic overview of the relative size and organization of CEP120 and SPICE1. In grey are the three C2 domains of CEP120. The other colors depict different structural elements: blue is a disordered or unknown region and green is a (predicted) coiled-coil domain. The ruler at the top indicates amino acid positions. Modified from Sharma et al., 2021. (B) The AlphaFold structure prediction of CEP120. The coiled-coil domain and the three C2 domains are visible. The colors indicate the model confidence: blue is very high confidence; red is very low confidence. (C) The AlphaFold structure prediction of SPICE1. There are multiple α-helices, and the two darker blue α-helices in the middle and on the top right are predicted coiled-coil domains. The colour-coding is the same as in (B) (Jumper et al., 2021).

domains are built from an eight-stranded antiparallel β-sandwich (Figure 2A). These domains were initially thought to be involved in Ca^{2+}-dependent membrane binding. Later it was found that the C2 domain can also be involved in protein-protein interactions (Cho & Stahelin, 2006). The C2A domain of CEP120 is the microtubule-binding domain, and the C2C domain is the domain through which CEP120 can interact with CPAP. Besides the C2 domains, CEP120 was also found to have a coiled-coil dimerization domain (Figure 2A). A coiled-coil is a secondary structure formed by two or more α-helices which entwine to form a cable structure. CEP120 has one α-helix and can form a homodimer with this domain (Sharma et al., 2018). Besides the interaction of CEP120 with CPAP, it can also interact with SPICE1. Since CPAP also promotes centriole elongation, all of these proteins have a shared function in centriole length control and cooperate during centriole elongation (Comartin et al., 2013). While the complete structure of CEP120 is not yet uncovered, a computationally predicted structure from AlphaFold is available (Figure 2B). In this structure, the three C2 domains and the coiled-coil domain are visible. Overall, while some aspects of CEP120 are known, its role and mechanism in centriole biogenesis are not yet completely understood.

Centriolar protein SPICE1

Spindle and centriole-associated protein 1 (SPICE1) was identified as a centriolar protein by proteomic analysis of the human centrosome (Andersen et al., 2003). Further study revealed that it localizes to the centrioles throughout the cell cycle and to spindle microtubules during mitosis. Staining for SPICE1 and centrin suggested that SPICE1 is present on the proximal end of the centriole. But the exact position on the centriole is not yet uncovered (Figure 1C). Furthermore, SPICE1 is required for centriole duplication and loss of SPICE1 causes short centrioles and mitotic defects because of impaired centriole duplication (Archinti et al., 2010). The structure of SPICE1 is not yet uncovered, but with the recent advancements in computational structure predictions, an AlphaFold structure prediction of the protein is available (Figure 2C). This structure shows that SPICE1 has a lot of disordered regions, which can complicate the research into this protein. It can make it harder to purify, resolve the structure with protein crystallography, and determine the functions of individual domains of the protein. However, for unstructured proteins or regions, it is known that they can become structured when bound, for example, to their interaction partner. Before the AlphaFold structure was available, two coiled-coil domains (CC1 and CC2) were already predicted (Figure 2A). They were predicted to be at amino acid positions 325-437 and 725-751. The AlphaFold structure has, aside from a lot of other α-helices, two α-helices at these positions. As mentioned previously, SPICE1 can interact with CEP120 and have a shared function. However, the function and mechanism of SPICE1 in centriole biogenesis remain unclear.

In vitro reconstitution experiments with CEP120 and SPICE1

There are multiple ways to characterize a protein. Various proteins involved in centriole biogenesis were uncovered by mass-spectrometry-based proteomic analysis and cellular experiments (knock out or knockdown) (Jakobsen et al., 2011). However, to complement the insights from these cellular experiments on the role of the protein of interest and its mechanism, the bottom-up approach of in vitro reconstitution experiments is beneficial. The cell is a crowded environment, and therefore, it is more complicated to see how individual components interact and affect a specific process. In this bottom-up approach, it is possible to study the effect of every individual component that is added. The understanding of microtubule dynamics, for example, has benefited significantly from in vitro reconstitution approaches.

In these experiments, cellular microtubule dynamics are studied in an in vitro model and visualized with super-resolution total internal reflection (TIRF) microscopy to analyze the microtubules' dynamics (Figure 3A). The primary behavior of microtubules growth and shrinkage is already visible in reconstitution assays with only purified tubulin. But with this model, complexity can be built to understand the role of a protein by introducing purified proteins of interest (Figure 3B). With this in vitro reconstitution approach, processes like microtubule aging, GTP-tubulin islands in the microtubule lattice, and mechanical tension on microtubules were uncovered (Akhmanova & Stearns, 2013). It became possible to understand these processes better than with cellular experiments alone. However, microtubule dynamics in a cellular environment are far more complex due to the many microtubule-associated proteins (MAPs) (Akhmanova & Steinmetz, 2008). But this effect of the MAPs also makes it hard to discern the impact of one of them in a cellular environment. Over the last few years, in vitro reconstitution assays have become an important tool to elucidate the function and mechanism of MAPs, especially since advances in the technique made it possible to study multiple MAPs at once and increase the system's complexity.

To analyze the microtubule dynamics, and thus also for the effect of MAPs, we look at the key parameters describing microtubules behavior such as the microtubule growth rate, microtubule shrinkage rate, catastrophe frequency, and rescue frequency (Zanic, 2016). Catastrophe of a microtubule is when the microtubule switches from growing to shrinking. When a catastrophe stops and the microtubule switches back from shrinking to growing, it is called rescue. Overall, in vitro reconstitution assays are a valuable tool in gaining insight into the function and mechanism of a MAP of interest.

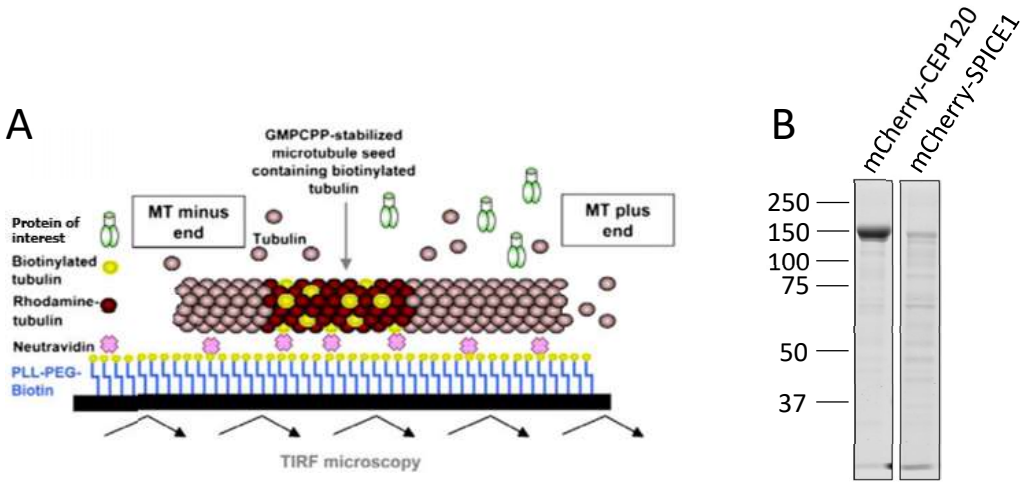

Figure 3. Schematic overview of an in vitro reconstitution experiment and the purified proteins of interest needed for in vitro reconstitution. (A) Schematic representation of an in vitro reconstitution assay setup. In an in vitro reconstitution assay, microtubules grow from a GMPCPP-stabilized microtubule seed. This seed is anchored to the coverslip via biotin-NeutrAvidin links. This makes it possible to image and analyze the dynamics of microtubules and the effect of different proteins. Adapted from Mohan et al., 2013. (B) SDS-PAGE of the purified CEP120 and SPICE1 proteins with mCherry-tag (~27 kDa). The ruler on the left indicates the size (kDa) of the proteins.

This study looked at how the interplay between CEP120 and SPICE1 plays a role in the centriole length control. Although CEP120 and SPICE1 are not conventionally seen as MAPs because they are centriolar proteins, they do interact with microtubules. So in vitro reconstitution assays would give insight into their function and mechanism. Firstly, we looked at CEP120 and SPICE1 behavior singly in the cellular environment and in in vitro reconstitution assays. In vitro reconstitution assays have never been done for both proteins, so this would give new information about their mechanism. Finally, we looked at the interactions and combined function of CEP120 and SPICE1. The interaction of both proteins has been reported to be important in centriole length regulation (Archinti et al., 2010; Comartin et al., 2013; Lin et al., 2013).

Materials & methods

DNA constructs, cell culture, and transfection

U2OS and HEK293T cells were cultured in Dulbecco's Modified Eagle Medium (DMEM) or DMEM/F10 (1:1 ratio) supplemented with 10% Fetal Bovine Serum (FBS) and 5 U/ml penicillin and 50 µg/ml streptomycin. CEP120 and SPICE1 expression constructs were made using cDNAs of the human proteins and cloning them into pEGFP-C1, mCherry-C1, and pTT5-C1 vectors by PCR-based cloning strategies. Additionally, a Strep-tag II (TGGAGCCACCCGCAGTTCGAAAAA) was introduced into the pTT5 vectors for protein purification purposes. The sequences of all constructed plasmids were confirmed. Cells were transfected with the various plasmids using FuGene6 (for imaging) or polyethylenimine (PEI, Polysciences) (for protein purification).

Antibodies, cell fixation, and immunofluorescence microscopy

Rat-anti-α-tubulin was used on fixed U2OS cells. For secondary antibodies, goat anti-rat conjugated with Alexa-405, Alexa-488, or Alexa-594 was used.

For tubulin staining, U2OS cells on coverslips were fixed in methanol at -20°C for 7 min. The cells were washed in PBS, permeabilized with PBS with 0.5% Triton X-100 for 10 min, and washed with PBS with 0.05% Tween 20 (PBST). The cells were blocked in 2% bovine serum albumin (BSA) in PBST and then incubated with the primary antibody. The cells were washed with PBST and incubated with the indicated secondary antibodies. Coverslips were rinsed with 70% and 90% ethanol and air-dried. The samples were mounted in Vectashield mounting media with DAPI staining (Vector Laboratories, Burlingame, CA).

Fixed cells were imaged with a Nikon Eclipse 80i upright fluorescence microscope equipped with a Plan Apo VC N.A. 1.40 oil 100x objective, Chroma ET-BFP2, -GFP or -mCherry filters, and a Photometrics CoolSNAP HQ2 CCD (Roper Scientific, Trenton, NJ) camera. The microscopes were controlled by Nikon NIS Br software.

Protein expression and purification from HEK293T cells for in vitro reconstitution assays

HEK293T cells were used to express and purify the proteins of interest. The cells were grown in DMEM/F10 (1:1 ratio) supplemented with 10% fetal bovine serum and 5 U/ml penicillin and 50 µg/ml streptomycin. Cells were transfected with pTT5 plasmids with GFP-CEP120, GFP-SPICE1, and mCherry-SPICE1 using PEI. An SII-tag was introduced to purify CEP120 and SPICE1. The cells were transfected with the respective plasmid DNA complexed at ratio 1:3 (w/w) with polyethyleneimine (1mg/mL) to form a PEI-DNA mixture in antibiotics free Ham's F10 nutrient mix (Gibco) for 30 minutes at room temperature. Afterwards, the PEI-DNA mixture was gently added to the adherent HEK293T cells in complete DMEM and incubated at 37˚C in a 5% CO2 incubator. Cells were harvested two days post-transfection. The cells from one 15 cm dish were lysed in 500 µl lysis buffer (50 mM HEPES, 300 mM NaCl, 0.5% Triton X-100, pH 7.4) supplemented with protease inhibitors (Roche). After clearing debris by centrifugation, cell lysates were incubated with 40 µl StrepTactin beads (GE Healthcare) per plate for 45 min. Beads were washed with lysis buffer without protease inhibitors. The proteins were eluted in 70 or 80 µl elution buffer (50 mM HEPES, 150 mM NaCl, 1mM MgCl2, 1 mM EGTA, 1 mM dithiothreitol (DTT), 2.5 mM d-Desthiobiotin and 0.05% Triton X-100, pH7.4). Elution was done three times to collect all the protein. Sample/supernatant was collected and stored at -80°C before use. The purity of the samples was analyzed via SDS-PAGE and Coomassie staining and with mass spectrometry. Concentrations of stock solutions varied from 1160 nM for GFP-CEP120 to 125-774 nM for GFP-SPICE1 and mCherry-SPICE1.

Mass spectrometry

To confirm the identity of purified proteins, purified protein samples were digested using S-TRAP microfilters (ProtiFi) according to the manufacturer's protocol. Briefly, 4 µg of protein sample was denatured in 5% SDS buffer and reduced and alkylated using DTT (20 mM, 10 min, 95°C) and IAA (40 mM, 30 min). Next, samples were acidified, and proteins were precipitated using a methanol TEAB buffer before loading on the S-TRAP column. Trapped proteins were washed four times with the methanol TEAB buffer and then digested overnight at 37°C using 1ug Trypsin (Promega). Digested peptides were eluted and dried in a vacuum centrifuge before LC-MS analysis.

Samples were analyzed by reversed-phase nLC-MS/MS using an Ultimate 3000 UHPLC coupled to an Orbitrap Q Exactive HF-X mass spectrometer (Thermo Scientific). Digested peptides were separated using a 50 cm reversed-phase column packed in-house (Agilent Poroshell EC-C18, 2.7 µm, 50cm x 75 µm) and were eluted at a flow rate of 300 nl/min using a linear gradient with buffer A (0.1% FA) and buffer B (80% ACN, 0.1% FA) ranging from 13-44% B over 38 min, followed by a column wash and re-equilibration step. The total data acquisition time was 55 min. MS data were acquired using a DDA method with the following MS1 scan parameters: 60,000 resolution, AGC target equal to 3E6, maximum injection time of 20 msec, the scan range of 375-1600 m/z, acquired in profile mode. The MS2 method was set at 15,000 resolution, with an AGC target set to standard, an automatic maximum injection time, and an isolation window of 1.4 m/z. Scans were acquired using a fixed first mass of 120 m/z and a mass range of 200-2000, and an NCE of 28. Precursor ions were selected for fragmentation using a 1-second scan cycle, a dynamic exclusion time set to 10 sec, and a precursor charge selection filter for ions possessing +2 to +6 charges.

Raw files were processed using Proteome Discoverer (PD) (version 2.4, Thermo Scientific). MSMS fragment spectra were searched using Sequest HT against a human database (UniProt, year 2020) that was modified to contain protein sequences from our cloning constructs and a common contaminants database. The search parameters were set using a precursor mass tolerance of 20 ppm and a fragment mass tolerance of 0.06 Da. Trypsin digestion was selected with a maximum of 2 missed cleavages. Variable modifications were set as methionine oxidation, and protein N-term acetylation and fixed modifications were set to carbamidomethylation. Percolator was used to assign a 1% false discovery rate (FDR) for peptide spectral matches, and a 1% FDR was applied to peptide and protein assemblies. An additional filter requiring a minimum Sequest score of 2.0 was set for PSM inclusion. MS1 based quantification was performed using the Precursor Ion Quantifier node with default settings applied. Precursor ion feature matching was enabled using the Feature Mapper node. Proteins matching the common contaminate database were filtered out from the results table.

In vitro reconstitution assay

The in vitro assays with dynamic microtubules were performed under the same conditions described previously (Sharma et al., 2016). GMPCPP-stabilized microtubule seeds were made and stored in MRB80 buffer (80 mM PIPES, pH 6.8, 4 mM MgCl2, 1 mM EGTA). Flow chambers were made with plasma-cleaned coverslips and microscopy slides. Coating was done with 0.2 mg/ml PLL-PEG-biotin (Susos AG, Switzerland) and 0.8 mg/ml NeutrAvidin (Invitrogen) in MRB80 buffer for 5 min each. Then the seeds were flushed in and attached to the coverslip via biotin-NeutrAvidin links. The seeds were blocked with 1 mg/ml κ-casein. Reaction mixtures consisting of MRB80 supplemented with 15 µM tubulin, containing 3% 562/647 labelled tubulin as indicated, 50 mM KCl, 0.1% methylcellulose, 0.2 mg/ml κ-casein, 1 mM GTP, oxygen scavenging system (20 mM glucose, 400 mg/ml glucose-oxidase), and the protein of interest in indicated concentration were added to the flow chamber after centrifugation in an Airfuge for 5 min at 119,000g. The flow chamber was sealed with vacuum grease, and dynamic microtubules were imaged immediately at 30˚C using a total internal reflection fluorescence (TIRF) microscope. All tubulin products were from Cytoskeleton Inc.

Total internal reflection fluorescence (TIRF) microscopy

TIRF imaging was performed on a microscope setup (inverted research microscope, Nikon Eclipse Ti-E), equipped with the perfect focus system (Nikon) and a Nikon CFI Apo TIRF 100/1.49 numerical aperture oil objective (Nikon). The microscope was supplemented with a TIRF-E motorized TIRF illuminator, modified by Roper Scientific/PICT-IBiSA Institut Curie, and a stage-top incubator (model no. INUBG2E-ZILCS, Tokai Hit) to regulate the temperature of the sample. Image acquisition was performed using a Photometrics Evolve 512 EMCCD camera (Roper Scientific) and controlled with MetaMorph7.7 software (Molecular Devices). The Evolve EMCCD camera's final resolution was 0.066 µ¬m/pixel. For excitation lasers, we used 491 nm 100 mW Stradus (Vortran), 561 nm 100 mW Jive (Cobolt) and 642 nm 110 mW Stradus (Vortran). We used an ET-GFP 49002 filter set (Chroma) for imaging proteins tagged with GFP, an ET-mCherry 49008 filter set (Chroma) for imaging X-Rhodamine labelled tubulin or mCherry- tagged proteins, and an ET647 for imaging Alexa647 labelled tubulin. We used sequential acquisition for the imaging experiments.

Analysis of microtubule dynamics in vitro

Kymographs were generated using the ImageJ plugin KymoResliceWide v.0.4 (https://github.com/ekatrukha/KymoResliceWide). Microtubule dynamics parameters were obtained from the kymographs. For the experiments determining the proportion of microtubule catastrophes or rescues, we manually observed the kymographs.

Results

CEP120 doesn't bind to microtubules but does bind to tubulin

To investigate the behavior of CEP120 in a cellular environment, we transfected U2OS with a GFP-CEP120 plasmid. When observed under the fluorescence upright microscope, we saw that CEP120 forms aggregates in highly expressing cells (Figure 4A). When a protein forms aggregates, it is most likely not functioning normally. Furthermore, CEP120 doesn't localize to the microtubules. The aggregation could be an overexpression issue. However, also in lower expressing cells, no microtubule-binding activity is observed (Figure 4A). So the microtubule-binding domain of CEP120 (C2A) is not functioning. In these lower expressing cells, CEP120 does localize to the centrioles like it should since CEP120 is a centriolar protein. In conclusion, these cellular experiments showed that CEP120 doesn't bind to the microtubule network but does localize to the centrioles.

When CEP120 is expressed together with CPAP, it becomes clear that CEP120 colocalizes and thus interacts with CPAP (Figure 4B). This confirms their interaction described in the literature. However, since they form aggregates, it is unlikely that they can perform their normal function in this situation. CPAP is also known to form aggregates on its own (Supplementary Figure 1). Aggregation is a problem with many centriolar proteins because they are expressed at very low levels in their normal cellular environment. However, the fact that CEP120 can still interact with CPAP showed that not all the functions of CEP120 are affected. CEP120 interacts with CPAP via its C2C domain, so this domain must still be functioning. Overall these cellular experiments showed that CEP120 localizes to the centrioles and interacts with CPAP but does not bind to the microtubule network.

To study the molecular mechanisms of CEP120 in in vitro reconstitution assays, we purified the protein to homogeneity using the same GFP-CEP120 protein construct as for the cellular work (Figure 3B and Supplementary Table 1). The average concentration of purified GFP-CEP120 was 1000 nM. As previously seen in U2OS cells, CEP120 did not bind to microtubules in vitro (Figure 4C, E). At a high concentration of 60 nM, it did not bind to the microtubules, but we observed it was aggregating like in the cellular environment. It is common for a protein to aggregate at a higher concentration. We tested it at lower concentrations and did not observe any microtubule-binding activity by CEP120 (Supplementary Figure 2). This is also in line with the cellular data. However, CEP120 did bind to free tubulin (Figure 4C). When we compared the dynamics of microtubules across the concentrations of CEP120 (10 nM, 20 nM and 60 nM) with microtubules from the control condition (15µM tubulin; Figure 4D), the growth rate remained unperturbed with increasing CEP120 concentration till 20 nM but almost became double (3.14 µm/min) at 60 nM (Figure 4F). The shortening rates were not affected across the concentrations (Figure 4G). The catastrophe frequency increased with increasing CEP120 concentration (Figure 4H).

To investigate the oligomeric state of CEP120, a single molecule count experiment was done. In this experiment, the fluorescent intensity of the protein of interest is compared to the fluorescent intensity of GFP – a known monomer – and EB3 – a known dimer. This revealed that CEP120 behaves as a dimer in solution (Figure 4I and Supplementary Table 3). CEP120 has a known coiled-coil dimerization domain. Thus, this experiment confirmed that CEP120 forms dimers.

SPICE1 binds to microtubules and forms a stabilizing zone

To investigate the role of SPICE1 in a cellular environment, we transfected U2OS cells with the GFP-SPICE1 plasmid and observed transfected cells under fluorescence upright microscopy. In highly expressing cells, SPICE1 binds to the microtubule network. We observed that SPICE1 is not present on all the microtubules in the cells but only on a subset (Figure 5A). In lower expressing cells, however, SPICE1 localizes to the centrioles. Localization to the centrioles is expected for SPICE1 since it is a centriolar protein. Overall, in contrast to CEP120, SPICE1 does bind to the microtubule network, but like CEP120, it localizes to the centrioles.

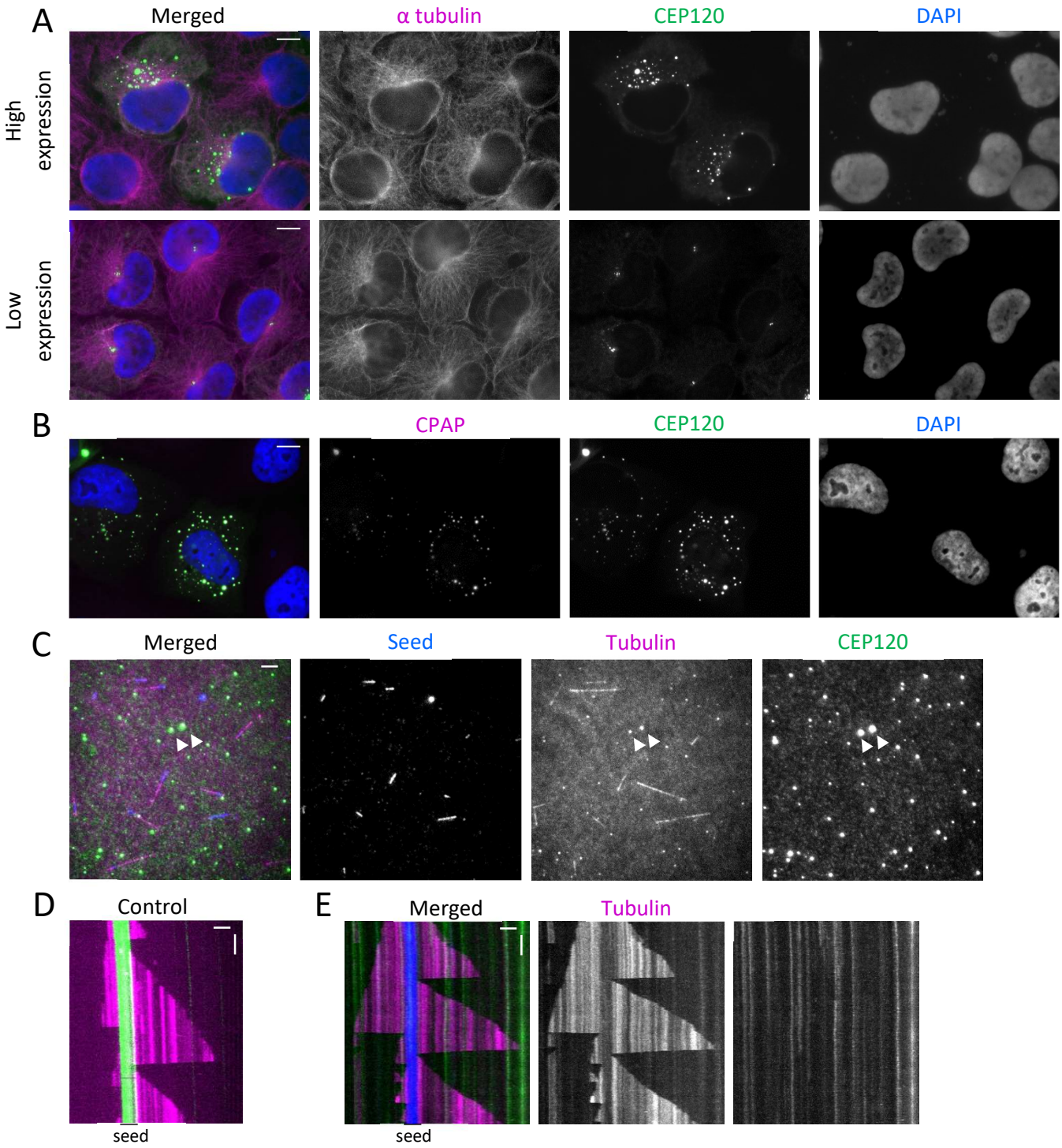

Description on the next page

Figure 4. CEP120 behavior in cellular and reconstitution assays. For the cellular experiments (A and B), the nucleus of the cells was stained with DAPI (blue). The scale bar is 10 µm. For the reconstitution assays (C-E), the tubulin and thus the microtubules are magenta; the protein of interest is in green (except for in the control). The horizontal scale bars are 2 µm and the vertical scale bars are 1 min. (A) GFP-CEP120 expressed in U2OS cells. The upper row shows cells that highly express the construct and in these cells CEP120 aggregates. The lower row shows cells with low expression levels and in these cells, and here CEP120 localizes to the centrioles. (B) GFP-CEP120 and CPAP-mCherry expressed together in U2OS cells. Although aggregates are formed, it is still clear by their localization that the two proteins interact. (C) A still from a movie of an in vitro reconstitution assay with 60 nM CEP120. The CEP120 doesn't bind to the microtubules but forms aggregates. The arrowheads indicate aggregates of CEP120 and tubulin, indicating that CEP120 binds to tubulin. (D) Kymograph with only tubulin (magenta) and stabilized seed (green) as the control condition. (E) Kymograph of 60 nM CEP120 showing no microtubule binding. (F) Analysis of the growth rate (G) shortening rate, and (H) catastrophe frequency for CEP120 reconstitution assays. (I) The single-molecule count experiment of CEP120 shows that CEP120 behaves as a dimer in solution.

To study the mechanism of SPICE1, we purified it to homogeneity (Figure 3B and Supplementary Table 2) and tested it with in vitro reconstitution assays (Figure 5B, C). In the in vitro assays, SPICE1 exhibited the same behavior as previously seen in the U2OS cells, i.e. it binds to microtubules. However, at a low concentration of SPICE1, it only binds to the microtubules and there is no discernable difference in microtubule growth rate compared to the control condition (15µM tubulin) (Figure 4D and 5B). With increasing concentrations of SPICE1, the effect on dynamic microtubules becomes more pronounced (Figure 5C and Supplementary Figure 3). Also, in the kymographs, it is visible that SPICE1 reduces the shortening rate and increases the rescue frequency. And at 50 nM of SPICE1, the protein binds the whole microtubule lattice (Figure 5C). SPICE1 stabilizes microtubules at this high concentration by forming a stabilizing zone on the microtubule that rescues it in case of a catastrophe. When a catastrophe occurs, SPICE1 can backtrack the microtubule, slow down the shortening, and eventually stop the catastrophe, allowing the microtubule to grow again. A SPICE1 stabilizing zone is a zone of more concentrated SPICE1 on the microtubule that prevents catastrophe. It starts forming when the microtubule is shrinking by attracting more SPICE1, which backtracks the microtubule. After the formation of this SPICE1 stabilizing zone, the microtubule can't shrink past it. This increased rescue capacity also causes the microtubules to become more processive. When the microtubule dynamics are analyzed, it becomes even more clear that the microtubule shortening rate decreases with increasing SPICE1 concentration (Figure 5E). The growth rate, however, is not affected by SPICE1 (Figure 5D). Analysis of the catastrophe frequency shows that it increases with increasing SPICE1 concentration (until 14 nM) and decreases again with even higher SPICE1 concentration (Figure 5F). Furthermore, the rescue frequency increases with increasing SPICE1 concentration, which is also what the kymographs showed (Figure 5G). Overall, there is a clear stabilizing effect of SPICE1 on the microtubules.

To investigate the oligomeric state of SPICE1, another single-molecule count experiment was done. This revealed that both SPICE1, like CEP120, behaves as a dimer in solution (Figure 5H and Supplementary Table 4). SPICE1 has two predicted coiled-coil domains. Thus, it is expected that this protein can form dimers.

SPICE1 recruits CEP120 to the microtubules

To investigate the interaction between CEP120 and SPICE1, we overexpressed both proteins in U2OS cells and did in vitro reconstitution assays with both proteins. When SPICE1 is expressed together with CEP120, SPICE1 can recruit the previously non-microtubule-binding CEP120 to the microtubules (Figure 6A), suggesting CEP120 interacts with SPICE1. Additionally, it is interesting that CEP120 doesn't form aggregates anymore, while it still did that when interacting with CPAP. This indicates that the interaction between SPICE1 and CEP120 is stronger than the interaction of CEP120 with itself, which caused the aggregates. Overall, these cellular experiments show that SPICE1 can recruit CEP120 to the microtubule network in cells.

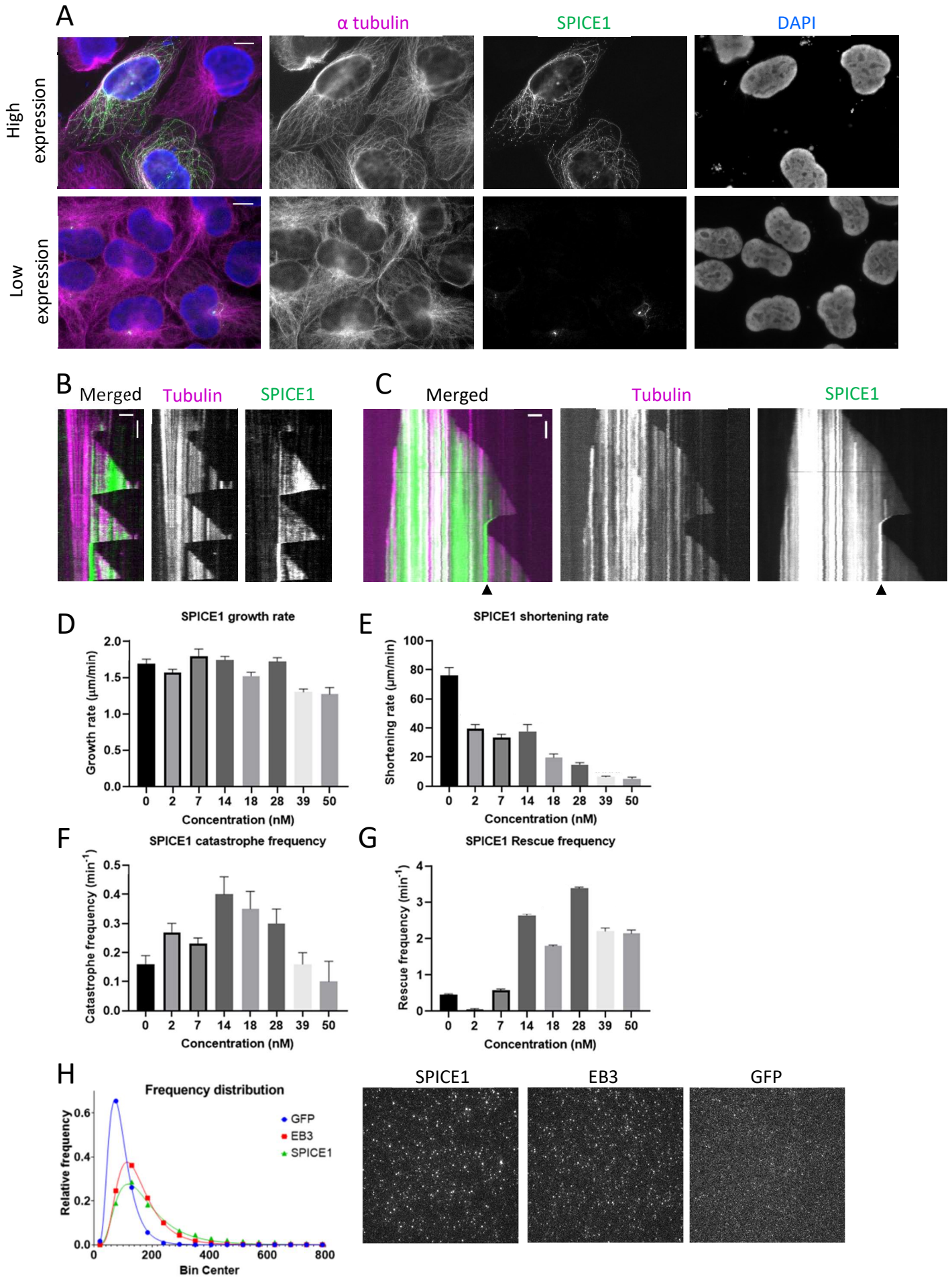

Figure 5. SPICE1 behavior in cellular and reconstitution assays. For the reconstitution assays (B and C), the tubulin and thus the microtubules are magenta; the protein of interest is in green. (continued on the next page)

The horizontal scale bars are 2 µm and the vertical scale bars are 1 min. (A) GFP-SPICE1 expressed in U2OS cells. The upper row shows cells with high expression levels and in these cells, SPICE1 binds to the microtubule network. The lower row shows lower expressing cells that have too little SPICE1 to bind to the whole microtubule network, but here SPICE1 localizes to the centrioles. (B) Kymograph of 7 nM SPICE1 showing microtubule-binding but no difference in dynamics compared to the control. (C) Kymograph of 50 nM SPICE1 showing microtubule binding and also an effect on dynamics with backtracking and rescue. The arrowheads indicate the SPICE1 stabilizing zone. (D) Analysis of the growth rate, (E) shortening rate, (F) catastrophe frequency, and (G) rescue frequency for SPICE1 reconstitution assays. (H) The single-molecule count experiment of SPICE1 shows that SPICE1 behaves as a dimer in solution.

Next, we looked to understand how the interaction between CEP120 and SPICE1 affects microtubule dynamics in vitro. For this, we used one stable SPICE1 concentration (39 nM) and added different concentrations of CEP120 (10, 20, and 60 nM) to see the effect of CEP120. Interestingly, in the in vitro reconstitution assays, SPICE1 also recruits CEP120 to the microtubule lattice, like in the cellular environment (Figure 6B). Furthermore, CEP120 seems to be present in higher concentrations at the spots where SPICE1 is also present in higher concentrations. For example, at the SPICE1 stabilizing zone that still forms in the presence of CEP120, SPICE1 and CEP120 are both more concentrated. Similar to the assays with only SPICE1, the microtubules become more processive because they get rescued. The shortening rate is lower than the control (15µM tubulin), like with only SPICE1, with all CEP120 concentrations (Figure 6D). Thus CEP120 doesn't affect the shortening rate of SPICE1 covered microtubules. CEP120 also didn't affect the shortening rate in assays with only CEP120. For the catastrophe frequency, there is an effect from CEP120 (Figure 6E). With lower CEP120 concentration (and stable SPICE1 concentration), CEP120 decreases the catastrophe frequency. But at a higher CEP120 concentration, the catastrophe frequency becomes higher than with SPICE1 alone. In the previous assays with CEP120 alone, we also saw that CEP120 increases the catastrophe frequency. The growth rate is not affected by CEP120 and remains the same as for SPICE1 alone (Figure 6C), while CEP120 alone did seem to increase the growth rate. Lastly, there is no clear effect of CEP120 on the rescue frequency (Figure 6F).

Overall, it is clear that CEP120 interacts with SPICE1 because we see this in the cellular environment and the in vitro reconstitution assays. Even though CEP120 alone could not bind to the microtubules, SPICE1 can recruit it to the microtubules. This interaction was previously reported to be important for centriole biogenesis. These new insights into how these proteins both individually and together affect microtubule dynamics bring us one step closer to understanding their mechanism in centriole biogenesis.

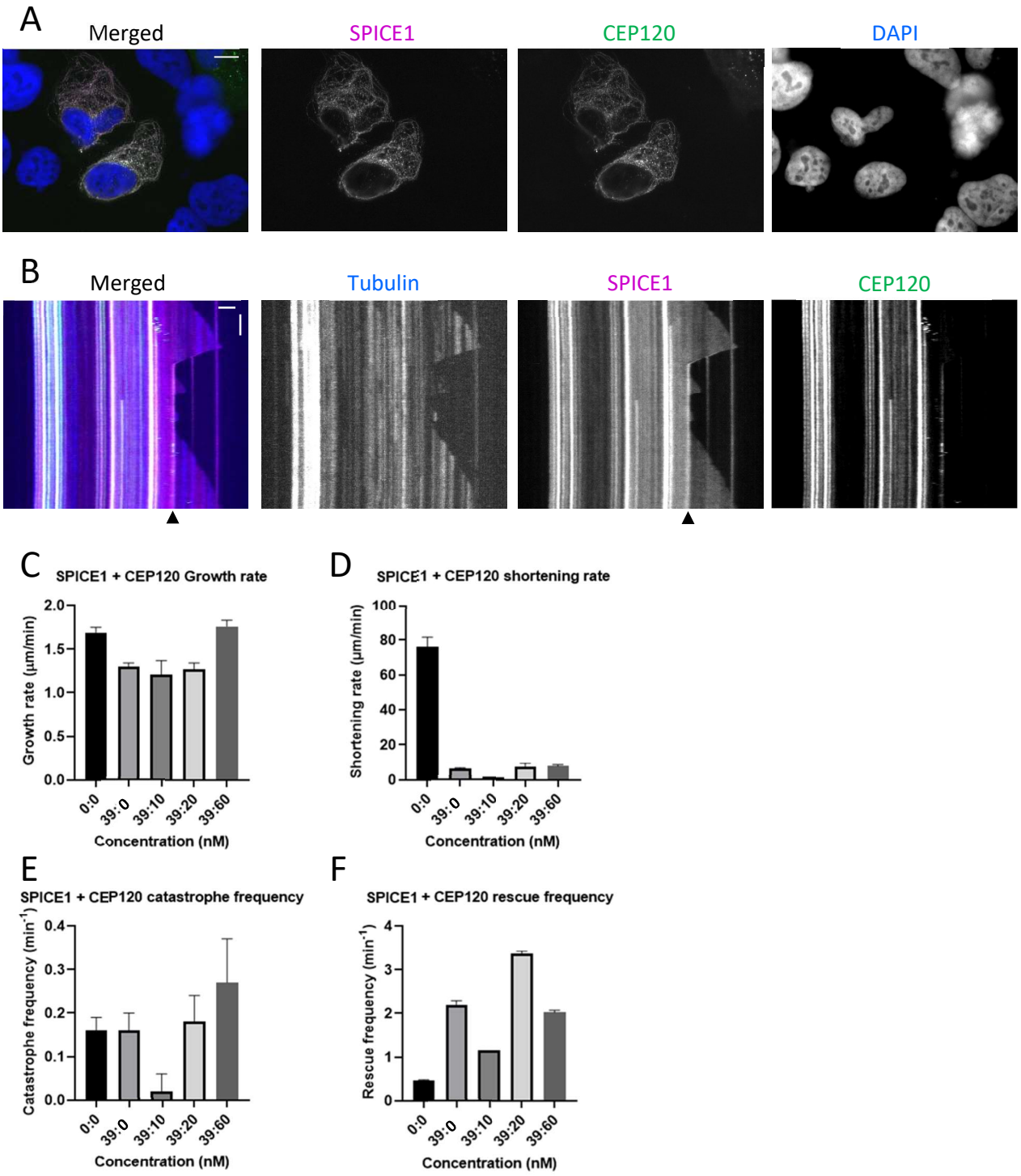

Figure 6. CEP120 and SPICE1 interaction in cellular and reconstitution assays. (A) Overexpression of GFP-CEP120 (green) and mCherry-SPICE1 (magenta) together in U2OS cells. SPICE1 recruits CEP120 to the microtubule network. The nucleus was stained with DAPI (blue). The scale bar is 10 µm. (B) Kymograph of 39 nM SPICE1 and 60 nM CEP120 where both proteins bind to the microtubule. The arrowheads indicate the SPICE1 stabilizing zone. The horizontal scale bar is 2 µm and the vertical scale bar is 1 min. (C) Analysis of the growth rate, (D) shortening rate, (E) catastrophe frequency, and (F) rescue frequency for CEP120 and SPICE1 reconstitution assays.

Discussion

To understand the function of centriolar proteins CEP120 and SPICE1, we looked at both proteins separately and together in the cellular environment and with in vitro reconstitution assays. Our data confirmed both CEP120 and SPICE1 as centriolar proteins (Banterle & Gönczy, 2017). Both proteins localized to the centriole at a low expression level in cellular assays. When expressed at a higher level, SPICE1 binds to a subset of cytosolic microtubules while CEP120 form cytosolic aggregates with no trace of microtubule-binding activity. The latter observation is at variance with previous literature reports of CEP120 binding to microtubules (Lin et al., 2013; Sharma et al., 2018). One explanation for the difference could be that CEP120 needs a partner to localize to the microtubules. Our in vitro experiments confirmed that SPICE1 is such a fiducial partner. This would deviate from previous findings where CEP120 could localize to the microtubule network in U2OS cells without the addition of SPICE1. However, this could be ascribed to the instability of cellular experiments. Protein concentrations can differ between cells without us knowing. And since CEP120 still maintained all of its other functions (tubulin-binding, dimerization, and interaction with CPAP and SPICE1), it would be hard to say only its microtubule-binding is affected.

An alternate argument could be that our protein construct was not functional because the predicted microtubule-binding domain (C2A) is at the N-terminus of the CEP120 protein, and our GFP-tag that was introduced at the N-terminus could have affected this domain. Thus the binding ability of the protein is compromised. However, although this GFP-tagged CEP120 construct couldn't bind to microtubules, it still localizes to the centrioles, binds to free tubulin, interacts with CPAP, is recruited to the microtubules by SPICE1, and behaves as a dimer in solution.

In in vitro assays, CEP120 didn't bind to dynamic microtubules, but the in vitro reconstitution revealed that CEP120 binds to free tubulin, thus highlighting that the C2A domain does seem to have some function left. It is reasonable to assume that the microtubule-binding domain is also the domain that binds to tubulin. It is also possible that the N-terminal GFP-tag only affected the ability to bind to microtubules and not to tubulin. Or, like mentioned above, CEP120 needs a partner to bind to microtubules, but apparently, it can bind to tubulin independently. Although CEP120 doesn't bind to the microtubules, it does affect the microtubule dynamics. It could be possible that the tubulin-binding or sequestration effect of CEP120 affects the microtubule dynamics by aggregating the tubulin so that it is not available for building the microtubules.

SPICE1, on the contrary, did bind microtubules both in vitro and in the cell. Previous work only showed localization to the centrosome and spindle microtubules during mitosis (Archinti et al., 2010). However, we saw SPICE1 localized to the microtubule network also outside mitosis in our experiments. Furthermore, the in vitro reconstitution assays suggest SPICE1 must have a microtubule-binding domain because it can bind microtubules in the reconstitution assays when only SPICE1 is added. SPICE1 only decorated a subset of the microtubules in the cell when overexpressed. We think it may be that its concentration may be suboptimal and hence that there is just too little SPICE1 to bind to all the microtubules. In the alternative, it could also be that SPICE1 has a preference for specific microtubules since microtubules can differ in their post-translational modifications (PTMs). Microtubules can have different PTMs and this impacts their dynamics and stability. The PTMs can also affect protein binding affinity to the microtubules (Jansen et al., 2021). To gain more insight into whether SPICE1 indeed has a preference for a specific subset of microtubules, additional research is needed.

Another important find is the stabilizing function of SPICE1 on the microtubules in vitro. One can see how this stabilizing function could be important in the biogenesis and preservation of the centriole length and architecture. However, the mechanism of how SPICE1 stabilizes the microtubules is still unknown. To further investigate the stabilizing function of SPICE1, an in vitro reconstitution assay with the microtubule polymerization inhibiting drug colchicine could be valuable. Colchicine promotes microtubule catastrophe, and thus, it would be interesting to see if SPICE1 can rescue these

catastrophes and, in this way, test the stabilizing effect of SPICE1. Since the stabilizing effect is of interest for its function in the centriole, it is advantageous to understand it better.

Furthermore, our in vitro assay confirmed previous findings by Comartin et al., 2013 that SPICE1 interacts with CEP120. Both proteins are required for centriole elongation. The recruitment of CEP120 to the microtubules by SPICE1 in the cell indicates that both proteins have a domain with which they can interact with each other. Our in vitro assays with CEP120 and SPICE1 combined showed that SPICE1 alone could recruit CEP120 to the microtubules and no other protein is needed for this. In addition, SPICE1 can interact with microtubules and CEP120 simultaneously, implying that these are two separate domains of SPICE1.

Interestingly, SPICE1 also behaves as a dimer in solution. While there is a predicted 3D model of SPICE1, the actual structure of this protein is still unknown. From available models, SPICE1 has two predicted coiled-coil domains. A coiled-coil domain often facilitates oligomerization, so it is expected that the coiled-coil domain of SPICE1 is the dimerization domain. However, having an experimentally solved structure could help explain better its properties, such as its oligomerization, the microtubule-binding and centriolar MAP binding behavior. With further research, a model of how SPICE1 interacts with CEP120 and binds to the microtubules and forms a stabilizing zone could be developed. This study characterized centriolar proteins CEP120 and SPICE1 and their interaction. The observed interaction between both proteins in cells and in in vitro reconstitution assays brings us a step closer to understanding their shared function in centriole biogenesis. Furthermore, the stabilizing effect of SPICE1 on microtubules and the interaction of centriolar proteins CEP120 and SPICE1 shed light on part of the complex process of centriole biogenesis.

References

Akhmanova, A., & Stearns, T. (2013). Cell architecture: Putting the building blocks together. *Current Opinion in Cell Biology*, *25*(1), 3–5. https://doi.org/10.1016/j.ceb.2012.12.003

Akhmanova, A., & Steinmetz, M. O. (2008). Tracking the ends: A dynamic protein network controls the fate of microtubule tips. *Nature Reviews Molecular Cell Biology*, *9*(4), 309–322. https://doi.org/10.1038/nrm2369

Andersen, J. S., Wilkinson, C. J., Mayor, T., Mortensen, P., Nigg, E. A., & Mann, M. (2003). Proteomic characterization of the human centrosome by protein correlation profiling. *Nature*, *426*(6966), 570–574. https://doi.org/10.1038/nature02166

Archinti, M., Lacasa, C., Teixidó-Travesa, N., & Lüders, J. (2010). SPICE – a previously uncharacterized protein required for centriole duplication and mitotic chromosome congression. *Journal of Cell Science*, *123*(18), 3039–3046. https://doi.org/10.1242/jcs.069963

Azimzadeh, J. (2014). Exploring the evolutionary history of centrosomes. *Philosophical Transactions of the Royal Society B: Biological Sciences*, *369*(1650), 20130453. https://doi.org/10.1098/rstb.2013.0453

Azimzadeh, J., & Marshall, W. F. (2010). Building the centriole. *Current Biology: CB*, *20*(18), R816-825. https://doi.org/10.1016/j.cub.2010.08.010

Banterle, N., & Gönczy, P. (2017). Centriole Biogenesis: From Identifying the Characters to Understanding the Plot. *Annual Review of Cell and Developmental Biology*, *33*(1), 23–49. https://doi.org/10.1146/annurev-cellbio-100616-060454

Bornens, M. (2012). The centrosome in cells and organisms. *Science (New York, N.Y.)*, *335*(6067), 422–426. https://doi.org/10.1126/science.1209037

Boveri, T. (2008). Concerning the Origin of Malignant Tumours by Theodor Boveri. Translated and annotated by Henry Harris. *Journal of Cell Science*, *121*(Supplement_1), 1–84. https://doi.org/10.1242/jcs.025742

Cho, W., & Stahelin, R. (2006). Membrane binding and subcellular targeting of C2 domains. *Biochimica et Biophysica Acta (BBA) - Molecular and Cell Biology of Lipids*, *1761*(8), 838–849. https://doi.org/10.1016/j.bbalip.2006.06.014

Comartin, D., Gupta, G. D., Fussner, E., Coyaud, É., Hasegan, M., Archinti, M., Cheung, S. W. T., Pinchev, D., Lawo, S., Raught, B., Bazett-Jones, D. P., Lüders, J., & Pelletier, L. (2013). CEP120 and SPICE1 Cooperate with CPAP in Centriole Elongation. *Current Biology*, *23*(14), 1360–1366. https://doi.org/10.1016/j.cub.2013.06.002

Fu, J., Hagan, I. M., & Glover, D. M. (2015). The centrosome and its duplication cycle. *Cold Spring Harbor Perspectives in Biology*, *7*(2), a015800. https://doi.org/10.1101/cshperspect.a015800

Gönczy, P. (2012). Towards a molecular architecture of centriole assembly. *Nature Reviews Molecular Cell Biology*, *13*(7), 425–435. https://doi.org/10.1038/nrm3373

Hildebrandt, F., Benzing, T., & Katsanis, N. (2011). Ciliopathies. *The New England Journal of Medicine*, *364*(16), 1533–1543. https://doi.org/10.1056/NEJMra1010172

Jakobsen, L., Vanselow, K., Skogs, M., Toyoda, Y., Lundberg, E., Poser, I., Falkenby, L. G., Bennetzen, M., Westendorf, J., Nigg, E. A., Uhlen, M., Hyman, A. A., & Andersen, J. S. (2011). Novel asymmetrically localizing components of human centrosomes identified by complementary proteomics methods. *The EMBO Journal*, *30*(8), 1520–1535. https://doi.org/10.1038/emboj.2011.63

Jansen, K. I., Burute, M., & Kapitein, L. C. (2021). *A live-cell marker to visualize the dynamics of stable microtubules* [Preprint]. Cell Biology. https://doi.org/10.1101/2021.06.23.449589

Joseph, N., Al-Jassar, C., Johnson, C. M., Andreeva, A., Barnabas, D. D., Freund, S. M. V., Gergely, F., & van Breugel, M. (2018). Disease-Associated Mutations in CEP120 Destabilize the Protein and Impair Ciliogenesis. *Cell Reports*, *23*(9), 2805–2818. https://doi.org/10.1016/j.celrep.2018.04.100

Jumper, J., Evans, R., Pritzel, A., Green, T., Figurnov, M., Ronneberger, O., Tunyasuvunakool, K., Bates, R., Žídek, A., Potapenko, A., Bridgland, A., Meyer, C., Kohl, S. A. A., Ballard, A. J., Cowie, A., Romera-Paredes, B., Nikolov, S., Jain, R., Adler, J., … Hassabis, D. (2021). Highly accurate protein structure prediction with AlphaFold. *Nature*, *596*(7873), 583–589. https://doi.org/10.1038/s41586-021-03819-2

Kellog, D. R., Moritz, M., & Alberts, B. M. (1994). The centrosome and cellular organization. *Annual Review of Biochemistry*, *63*, 639–674. https://doi-org.proxy.library.uu.nl/10.1146/annurev.bi.63.070194.003231

Klotz, C., Dabauvalle, M.-C., Paintrand, M., Weber, T., Bornens, M., & Karsenti, E. (1990). Parthenogenesis in Xenopus eggs requires centrosomal integrity. *The Journal of Cell Biology*, *110*(2), 405–415.

Lin, Y.-N., Wu, C.-T., Lin, Y.-C., Hsu, W.-B., Tang, C.-J. C., Chang, C.-W., & Tang, T. K. (2013). CEP120 interacts with CPAP and positively regulates centriole elongation. *Journal of Cell Biology*, *202*(2), 211–219. https://doi.org/10.1083/jcb.201212060

Mohan, R., Katrukha, E. A., Doodhi, H., Smal, I., Meijering, E., Kapitein, L. C., Steinmetz, M. O., & Akhmanova, A. (2013). End-binding proteins sensitize microtubules to the action of microtubule-targeting agents. *Proceedings of the National Academy of Sciences*, *110*(22), 8900–8905. https://doi.org/10.1073/pnas.1300395110

Nigg, E. A., & Raff, J. W. (2009). Centrioles, Centrosomes, and Cilia in Health and Disease. *Cell*, *139*(4), 663–678. https://doi.org/10.1016/j.cell.2009.10.036

Nogales, E. (2001). Structural insight into microtubule function. *Annual Review of Biophysics and Biomolecular Structure*, *30*, 397–420. https://doi.org/10.1146/annurev.biophys.30.1.397

Ohta, T., Essner, R., Ryu, J.-H., Palazzo, R. E., Uetake, Y., & Kuriyama, R. (2002). Characterization of Cep135, a novel coiled-coil centrosomal protein involved in microtubule organization in mammalian cells. *The Journal of Cell Biology*, *156*(1), 87–100. https://doi.org/10.1083/jcb.200108088

Paintrand, M., Moudjou, M., Delacroix, H., & Bornens, M. (1992). Centrosome organization and centriole architecture: Their sensitivity to divalent cations. *Journal of Structural Biology*, *108*(2), 107–128. https://doi.org/10.1016/1047-8477(92)90011-X

Roque, H., Wainman, A., Richens, J., Kozyrska, K., Franz, A., & Raff, J. W. (2012). Drosophila Cep135/Bld10 maintains proper centriole structure but is dispensable for cartwheel formation. *Journal of Cell Science*, *125*(23), 5881–5886. https://doi.org/10.1242/jcs.113506

Schatten, G., & Simerly, C. (2015). LEGOs® and legacies of centrioles and centrosomes. *EMBO Reports*, *16*(9), 1052–1054. https://doi.org/10.15252/embr.201540875

Schmidt, T. I., Kleylein-Sohn, J., Westendorf, J., Le Clech, M., Lavoie, S. B., Stierhof, Y.-D., & Nigg, E. A. (2009). Control of Centriole Length by CPAP and CP110. *Current Biology*, *19*(12), 1005–1011. https://doi.org/10.1016/j.cub.2009.05.016

Sharma, A., Aher, A., Dynes, N. J., Frey, D., Katrukha, E. A., Jaussi, R., Grigoriev, I., Croisier, M., Kammerer, R. A., Akhmanova, A., Gönczy, P., & Steinmetz, M. O. (2016). Centriolar CPAP/SAS-4 Imparts Slow Processive Microtubule Growth. *Developmental Cell*, *37*(4), 362–376. https://doi.org/10.1016/j.devcel.2016.04.024

Sharma, A., Gerard, S. F., Olieric, N., & Steinmetz, M. O. (2018). Cep120 promotes microtubule formation through a unique tubulin binding C2 domain. *Journal of Structural Biology*, *203*(1), 62–70. https://doi.org/10.1016/j.jsb.2018.01.009

Sharma, A., Olieric, N., & Steinmetz, M. O. (2021). Centriole length control. *Current Opinion in Structural Biology*, *66*, 89–95. https://doi.org/10.1016/j.sbi.2020.10.011

Silflow, C. D., & Lefebvre, P. A. (2001). Assembly and Motility of Eukaryotic Cilia and Flagella. Lessons from Chlamydomonas reinhardtii. *Plant Physiology*, *127*(4), 1500–1507.

Slep, K. C. (2016). The Secret of Centriole Length: Keep a LID on It. *Developmental Cell*, *37*(4), 293–295. https://doi.org/10.1016/j.devcel.2016.05.008

Tsai, J.-J., Hsu, W.-B., Liu, J.-H., Chang, C.-W., & Tang, T. K. (2019). CEP120 interacts with C2CD3 and Talpid3 and is required for centriole appendage assembly and ciliogenesis. *Scientific Reports*, *9*(1), 6037. https://doi.org/10.1038/s41598-019-42577-0

Uzbekov, R., & Alieva, I. (2018). Who are you, subdistal appendages of centriole? *Open Biology*, *8*(7), 180062. https://doi.org/10.1098/rsob.180062

Winey, M., & O'Toole, E. (2014). Centriole structure. *Philosophical Transactions of the Royal Society B: Biological Sciences*, *369*(1650), 20130457. https://doi.org/10.1098/rstb.2013.0457

Wu, J., & Akhmanova, A. (2017). Microtubule-Organizing Centers. *Annual Review of Cell and Developmental Biology*, *33*, 51–75. https://doi.org/10.1146/annurev-cellbio-100616-060615

Zanic, M. (2016). Measuring the Effects of Microtubule-Associated Proteins on Microtubule Dynamics In Vitro. In P. Chang & R. Ohi (Eds.), *The Mitotic Spindle* (Vol. 1413, pp. 47–61). Springer New York. https://doi.org/10.1007/978-1-4939-3542-0_4

Supplementary information

Supplementary Table 1. Mass spectrometry analysis of the purified CEP120 protein. The first ten hits and their UniProt accession number, gene name, coverage, and the number of unique peptides are listed.

Acccession	Description	Coverage [%]	# Unique Peptides
Q8N960	**Centrosomal protein of 120 kDa [CEP120]**	**90**	**136**
tagEGFP	tag EGFP	87	25
P04264	Keratin, type II cytoskeletal 1 [KRT1]	66	37
P0DMV9	Heat shock 70 kDa protein 1B [HSPA1B; HSPA1A]	65	33
P35527	Keratin, type I cytoskeletal 9 [KRT9]	78	42
P35908	Keratin, type II cytoskeletal 2 [KRT2]	74	1
P11142	Heat shock cognate 71 kDa protein [HSPA8]	62	25
P11182	Lipoamide acyltransferase component of branched-chain alpha-keto acid dehydrogenase complex, mitochondrial [DBT]	67	29
P07437	Tubulin beta chain [TUBB]	74	4
P68371	Tubulin beta-4B chain [TUBB4B]	73	1

Supplementary Table 2. Mass spectrometry analysis of the purified SPICE1 protein. The first ten hits and their UniProt accession number, gene name, coverage, and the number of unique peptides are listed.

Acccession	Description	Coverage [%]	# Unique Peptides
Q8N0Z3	**Spindle and centriole-associated protein 1 [SPICE1]**	**72**	**71**
P0DMV9	Heat shock 70 kDa protein 1B [HSPA1B; HSPA1A]	75	32
P04264	Keratin, type II cytoskeletal 1 [KRT1]	63	38
P11142	Heat shock cognate 71 kDa protein [HSPA8]	66	32
tagEGFP	tag EGFP	87	18
P35527	Keratin, type I cytoskeletal 9 [KRT9]	75	31
P11021	78 kDa glucose-regulated protein [HSPA5]	58	37
P17066	Heat shock 70 kDa protein 6 [HSPA6]	21	1
P35908	Keratin, type II cytoskeletal 2 epidermal [KRT2]	67	29
P11182	Lipoamide acyltransferase component of branched-chain alpha-keto acid dehydrogenase complex, mitochondrial [DBT]	61	28

Supplementary Table 3. The analysis of the single-molecule count experiment of CEP120. The amplitude, geometric mean, and geometric standard of GFP, EB3, and CEP120 are listed.

Lognormal	GFP	EB3	CEP120
Best-fit values			
A	186.8	147.4	152.0
GeoMean	506.0	833.8	787.2
GeoSD	1.516	1.721	1.687

Supplementary Table 4. The analysis of the single-molecule count experiment of SPICE1. The amplitude, geometric mean, and geometric standard of GFP, EB3, and SPICE1 are listed.

Lognormal	GFP	EB3	SPICE1
Best-fit values			
A	55.03	47.78	38.48
GeoMean	90.53	139.6	153.3
GeoSD	1.473	1.582	1.672

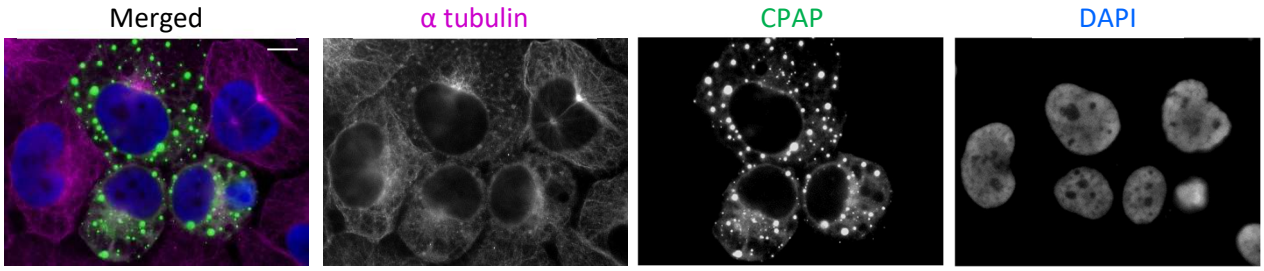

Supplementary Figure 1. CPAP-GFP overexpressed in U2OS cells. The nucleus of the cells was stained with DAPI (blue). The scale bar is 10 µm. CPAP is known to form aggregates at higher concentrations.

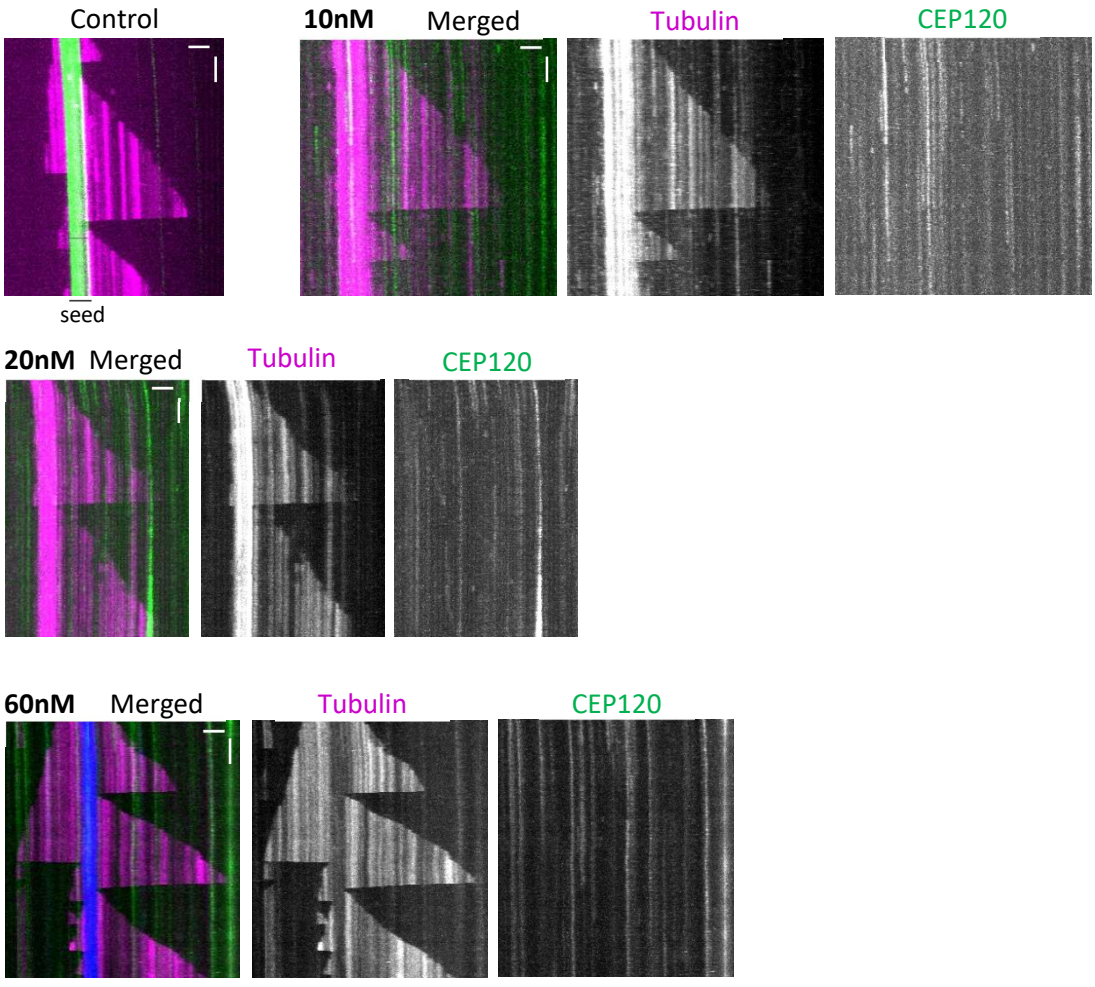

Supplementary Figure 2. Kymographs of all the CEP120 concentrations that were tested with in vitro reconstitution assays. The tubulin and thus the microtubules are magenta; the protein of interest is in green (except for in the control). The horizontal scale bars are 2 µm and the vertical scale bars are 1 min. CEP120 concentrations of 10, 20, and 60 nM were used. With all concentrations, no CEP120 microtubule-binding is observed.

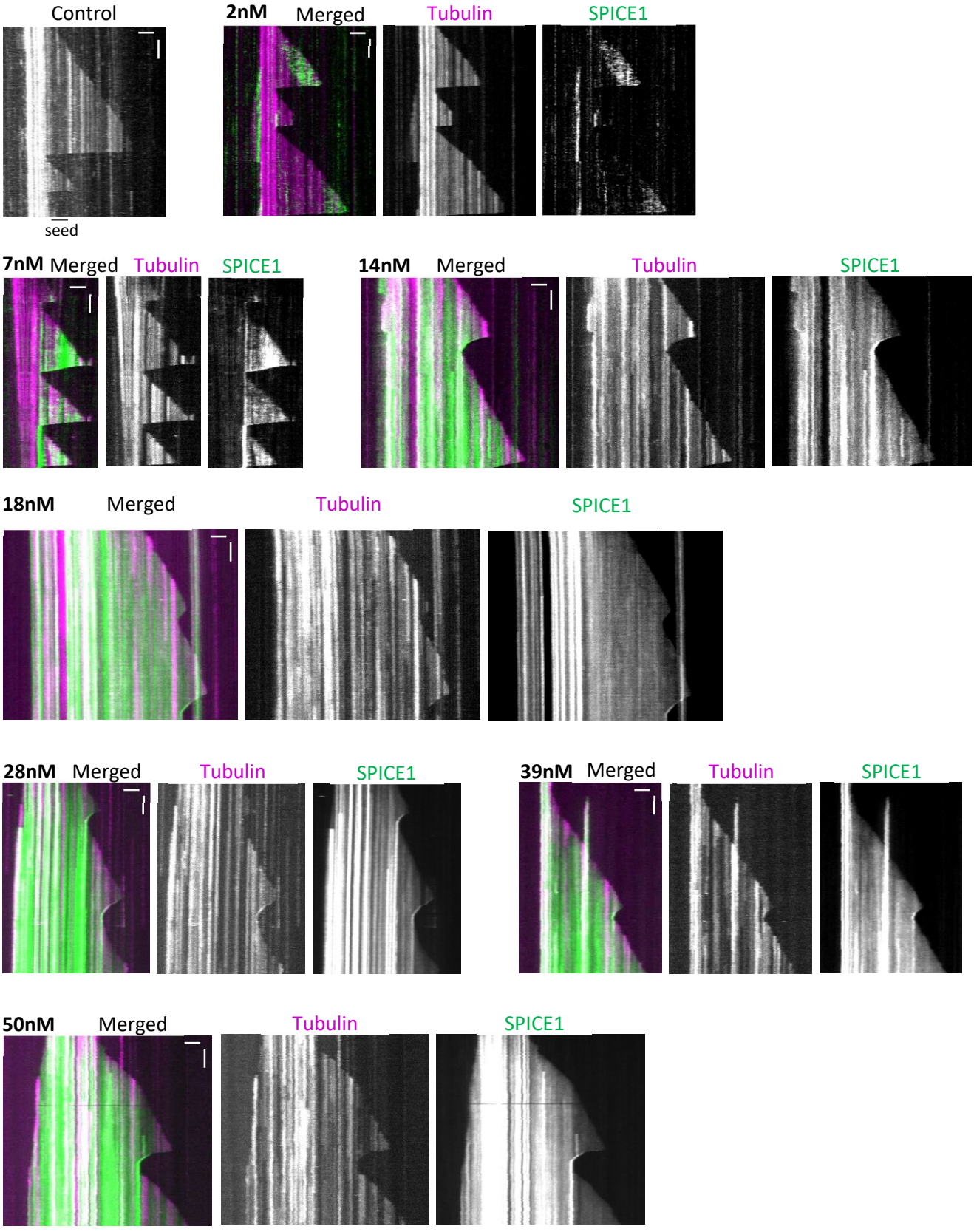

Supplementary Figure 3. Kymographs of all the SPICE1 concentrations that were tested with in vitro reconstitution assays. The tubulin and thus the microtubules are magenta; the protein of interest is in green (except for in the control). The horizontal scale bars are 2 µm and the vertical scale bars are 1 min. SPICE1 concentrations of 2, 7, 14, 18, 28, 39, and 50 nM were used. With increasing SPICE1-concentration, increasing SPICE1 microtubule-binding and stabilization is observed.